Conformational analysis investigation into the influence of nano-porosity of ultra-permeable ultra-selective polyimides on its diffusivity as potential membranes for use in the "green" separation of natural gases

Tarek M Madkour

The American University in Cairo (AUC), School of Sciences and Engineering, Department of Chemistry, AUC Avenue, P.O. Box 74, New Cairo 11835, Egypt

E-mail: tarek.madkour@aucegypt.edu

Abstract. Nano-porous polymers of intrinsic microporosity, PIM, have exhibited excellent permeability and selectivity characteristics that could be utilized in an environmentally friendly gas separation process. A full understanding of the mechanism through which these membranes effectively and selectively allow for the permeation of specific gases will lead to further development of these membranes. Three factors obviously influenced the conformational behavior of these polymers, which are the presence of electronegative atoms, the presence of non-linearity in the polymeric backbones (backbone kinks) and the presence of bulky side groups on the polymeric chains. The dipole moment increased sharply with the presence of backbone kinks more than any other factor. Replacing the fluorine atoms with bulky alkyl groups didn't influence the dipole moment greatly indicating that the size of the side chains had much less dramatic influence on the dipole moment than having a bent backbone. Similarly, the presence of the backbone kinks in the polymeric chains influenced the polymeric chains to assume less extended configuration causing the torsional angles around the interconnecting bonds unable to cross the high potential energy barriers. The presence of the bulky side groups also caused the energy barriers of the cis-configurations to increase dramatically, which prevented the polymeric segments from experiencing full rotation about the connecting bonds. For these polymers, it was clear that the fully extended configurations are the preferred configurations in the absence of strong electronegative atoms, backbones kinks or bulky side groups. The addition of any of these factors to the polymeric structures resulted in the polymeric chains being forced to assume less extended configurations. Rather interestingly, the length or bulkiness of the side groups didn't affect the end-to-end distance distribution to a great deal since the presence of quite large bulky side chain such as the pentyl group has caused the polymeric chains to revert back to the fully extended configurations possibly due to the quite high potential energy barriers that the chains have to cross to reach the less extended configurational states.

1. Introduction

Nanoporous materials are characterized with small pore sizes whose diameters can be adjusted and therefore can be used for gas mixture separations depending on their size exclusion [1]. It was also mentioned that the lower energy and cost needed for membrane-based gas separation techniques than traditional processes made the membrane methods more preferred [2,3]. It was illustrated that the

membranes must have certain properties such as high permeability, high selectivity, mechanical stability and low cost to be useful for gas mixture separation such as hydrogen and nitrogen gas mixture and the purification of natural gas through the removal of carbon dioxide [4]. Silicon rubber, cellulose acetate, polysulfone materials are all known to be used in case of O_2/N_2 separation, however polyimides are used for both O_2/N_2 and CO_2/CH_4 separations. Both the diffusivity and solubility parameters control the diffusion mechanism at which the mobility of the molecules is reflected by its diffusivity. It was claimed that the increase in the molecular size of the gas leads to reduction in the diffusion coefficient, and increasing in the solubility coefficient [5]. Enhancement in the diffusivity or the solubility leads to a decrease in the membrane selectivity since increasing the permeability occurs on the expense of the selectivity of the membranes. Glassy polymers of microporosity nature achieve high permeability/selectivity ratios that are close to the upper bound in the separation processes of simple gases, at which they allow the diffusion of smaller molecules more rapidly than larger ones. It was claimed [5] that the high selectivity and good mechanical properties are the reasons for using membranes formed by glassy polymers in gas separations. Rubbery polymers, however, are shown to be more effective in isolating bulky organic molecules from smaller gas molecules since rubbery membranes have high permeability with low selectivity.

Production of polymeric membranes with both high permeability and selectivity while maintaining long-term stability is considered a challenge. Polyimides of intrinsic microporosity are such examples [6]. It was claimed that the rigid and contorted macrostructures that are not able to pack space efficiently are the reason for their microporosity and high gas permeability, at which the rigidity is obtained by fused ring structure and the sites of contortion are made by spirocentres. It was also reported that these nanoporous polymeric materials are similar to glassy polymers but with higher solubility coefficient [7] which subsequently allows for permeability enhancement without selectivity loss. It is believed that these materials are excellent candidates as separation membranes for their high permeability, good selectivity and long thermal stability.

Polymers of intrinsic microporosity (PIMs) that were first created by Mckeown and Budd [8] were synthesized from rigid and bent monomers which have a tetrahedral carbon atom known as a "site of contortion" responsible for the porosity in PIMs. This site of contortion led to the observed free volume between the polymer chains. They also illustrated the different ways by which PIMs can be synthesized. Dioxine-forming reaction between an orthodihydroxy monomer and an orthodihalide monomer can be used to produce linear polymer. Interestingly, a network can be also synthesized if one of the monomers has more than two pairs of halides. Early microporous PIM networks were based on phthalocyanines and porphyrins and enclosed metal ions or 2H in the cavities. More Recent PIM networks were synthesized from a hexaazatrinaphythylene monomer, which made metal binding possible and contributed to greater mass that will eventually lead to a decrease in the surface area. Other PIMs could be synthesized by incorporating bis(phenazyl)s, fused fluorenes and imides, which led to a variety of gas permeability characteristics.

PIMs synthesized from rigid twisted spirobiflurones through imide- and amide-forming reactions showed the highest surface area and rigidity. The surface areas were somewhat low when the imide-forming reactions formed PIMs with binaphthalene as the site of contortion. Advanced polyimide forming reactions including binaphthalene and 4-4`-(9-fluorenylidene) dianiline were done and when the polymers were used as films, they exhibited selective CO_2/H_2 gas uptake. Hyper cross-linked polymers (HCPs) such as cross-linked polystyrene otherwise known as Davankov resins were created by the same way resulting in highly rigid networks that are characterized by small pore sizes, high surface areas and high resistance to collapsing [9]. They can be formed by the polymerization of vinylbenzyl chloride with a small amount of divinylbenzene cross-linker to form a lightly cross-linked copolymer. The copolymer is then allowed to be "hyper cross-linked" via a Fidel-craft alkylation reaction using a Lewis acid such as iron (III) chloride after being swollen in an appropriate solvent [10]. Germain et al. [11] created hyper crosslinking of linear polyaniline and polypyrole precursors, without requiring the use of lithiating agents or huge amounts of Lewis acids and consequently, it does

not produce large volumes of HCl gas [12]. Polyaniline can be cross-linked using Ullmann and Buchwald coupling reaction, leading to the formation of networks connected by aromatic groups. They also highlighted that thermodynamic compatible solvents used with the precursor led to faster desolvation during crosslinking. To determine the best solvent for a certain crosslinking process,
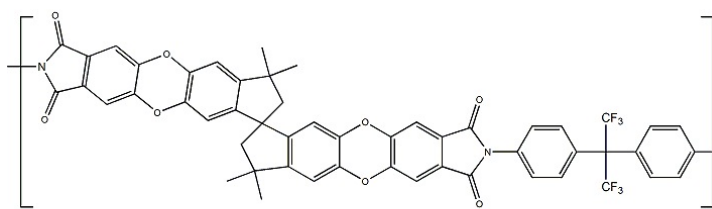
Table 1. Different molecular structures of the PIM-polyimides under investigation.
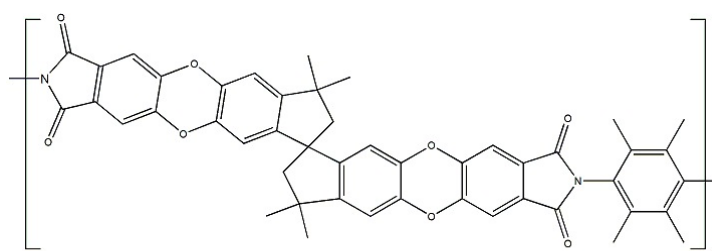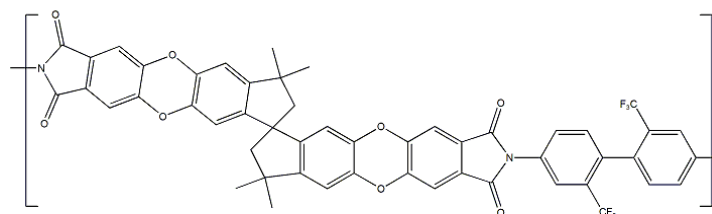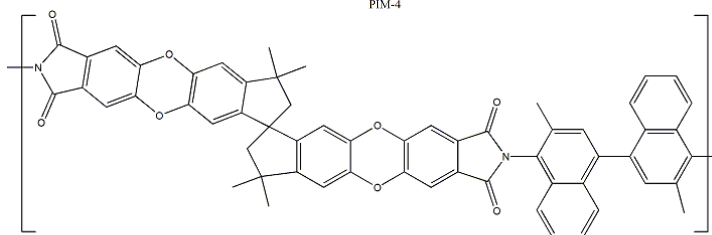

PIM-1
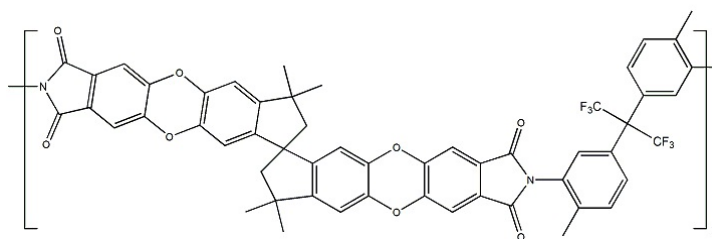
PIM-2

PIM-3

PIM-4

PIM-8

Hildebrand and Hansen parameters were used. Compatible monomer/solvent systems have similar values for the Hildebrand and Hansen parameters. The performed reaction should have fast chemical kinetics and results in the least amount of non-crosslinked by-products. Finally, there should be no chemical reaction between the reactant and the solvent since they may lead to the formation of two intermixed polymer networks [13].

2. Simulation methodology

2.1 The chemical structures of the investigated polymers

The polymeric structures simulated in this article are polyimides that are commonly prepared by a step polymerization involving a cycloimidization reaction between a bis(carboxylic anhydride) and a diamine. The investigated polyimides were synthesized and characterized by Ghanem et al [14]. The polymers showed excellent selectivity and permeability characteristics due to the high restriction for rotation around the imide linkage. According to the authors [14], to create even more permeable polyimides, the PIM concept was applied. A dianhydride was prepared that incorporated a spiro-centre, referred to as a centre of contortion. Table 1 illustrates the chemical structure of five different PIMs (PIM-1, PIM-2, PIM-3, PIM-4 and PIM-8) that were prepared and characterized experimentally by Ghanem et al [14] and chosen here to examine the influence of the polymeric chemical structure on the conformational behavior of the investigated polymer in relation to its experimentally determined permeability.

2.2 Choice of force field

All calculations were performed using Materials Studio® Package from Accelrys, inc. The quality of the forcefield, which consists of a set of analytical function terms and parameters, and provides a detailed description of the inter- and intramolecular interactions as a function of the molecular structures and their relative positions influences directly the reliability of the simulations to a great deal. The simulation of the different polymeric systems has been carried out using the COMPASS forcefield. The COMPASS forcefield is a CFF-type forcefield [15] constructed using exact ab-initio quantum mechanics calculations and developed to improve upon existing forcefields. In the forcefield approach, the potential energy of a system is expressed as a sum of valence and non-bonded interactions:

$$E_{total} = E_{valence} + E_{nonbond} = (E_{bond} + E_{angle} + E_{torsion} + E_{inv}) + (E_{vdW} + E_{Coulomb}) \tag{1}$$

The valence terms parameterize the short-range intramolecular interactions that determine the bond lengths (E_{bond}), bond angles (E_{angle}), torsion angles ($E_{torsion}$) and out-of-plane inversion angles (E_{inv}). The nonbonded interactions, which can be both intra- and intermolecular, are split into a dispersive van der Waals term (E_{vdW}), and electrostatic term ($E_{Coulomb}$). Other cross-terms are also important and well accounted for by the COMPASS forcefield.

2.3 Conformational Analysis

Various conformational properties of the investigated polymeric systems evaluated using RIS Metropolis Monte Carlo methods, RMMC, available through the Conformer module® as part of Materials Studio® Package from Accelrys, inc. [16-18]. Unlike traditional rotational isomeric states methods, RMMC methods allow torsion angles to vary continuously and therefore do not impose the assumption of discrete rotational states. The method is thus based on relative energies of the new and the old conformation. The bond-based cut-off method was used for the simulations of the single polymeric chains in the θ-condition. In this method, the parameters n_{min} and n_{max} affect the way van der Waals and Coulomb energies are evaluated in the RMMC simulation. The nonbond energies were not computed for atoms that are closer than n_{min} or further apart than n_{max}. The usual value for n_{min} was 3 whereas that of n_{max} was taken as 6 in order to include the interactions of the side chains of the neighbouring repeat units in the energy evaluation.

Table 2 lists the chemical structures of new compounds that have not been synthesized experimentally yet but envisaged to have good permeability characteristics and may assist in the further understanding through the conformational analysis of the origin of microporosity in these PIM-polyimides.

Table 2. Different molecular structures of new envisaged PIM-polyimides.

PIM-4-CH₃

PIM-4-C₃H₇

PIM-4-C₅H₁₁
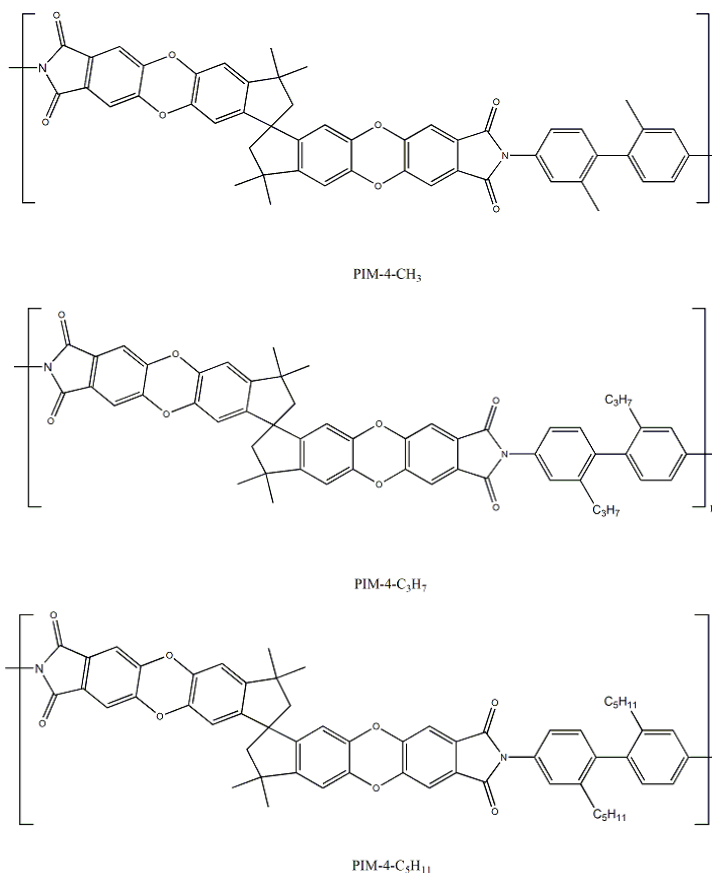
RMMC simulations were done for polymers with 100 repeat units at room temperature. The number of the equilibration steps was 10,000 for each rotatable bond. This stage was necessary to bring the polymer chain from its initial conformation to a conformation typical for the chain in the melt at the desired temperature. The number of simulation steps was 50,000 steps for each rotatable bond. The block-averaged values of the mean squared end-to-end distance and energy were plotted as functions of the simulation step number in order to determine if the system was fully equilibrated. There was no evidence of any long-term drift in mean squared end-to-end distance and energy over the course of simulation, which indicated that the chains had reached a steady state. RMMC was used to calculate the conformational parameters such as the dipole moment, the end-to-end distances and the radii of gyration. The end-to-end distance, r, of a single chain is defined as:

$$r = \sum_{i=1}^{n} l_i \qquad (2)$$

where l_i denotes the vector along backbone bond i, and n denotes the number of backbone bonds in the molecule. The radius of gyration, S, is defined as the root mean squared distance of the atoms in the molecule from their common centre of mass and is given by:

$$S^2 = \frac{\sum_{i=1}^{N} m_i s_i^{\,2}}{\sum_{i=1}^{N} m_i} \tag{3}$$

where S_i denotes the distance of atom i from the centre of mass, and N denotes the total number of atoms. The radial distribution function (RDF) gives a measure of the probability that, given the presence of an atom at the origin of an arbitrary reference frame, there will be an atom with its center located in a spherical shell of infinitesimal thickness at a distance r from the reference atom. The radial distribution function, $g_{\alpha\beta}(r)$, is calculated from the average of the static relationship of every given pair of particles, $\alpha\beta$, as:

$$C(m) = \frac{1}{n} \sum_{i=1}^{n} V(m+i) \times V(i) \tag{4}$$

where $<n_{\alpha\beta}(r)>$ is the average number of atom pairs in the spherical shell between r and r+Δr, $\alpha\beta$ denotes the possibility that α and β particles may be of a different chemical nature, and $\rho_{\alpha\beta}$ is the density of atom pairs of type $\alpha\beta$. By investigating the radial distribution function, more information on the local packing influenced by specific interactions could be obtained. To evaluate the influence of contortion of these polymers on its conformational behavior, the probability distribution function of the angle of contortion around the spiro-centre is evaluated. Figure 1a shows a schematic drawing illustrating the specified angle of contortion (θ_c).

(a)   **(b)**
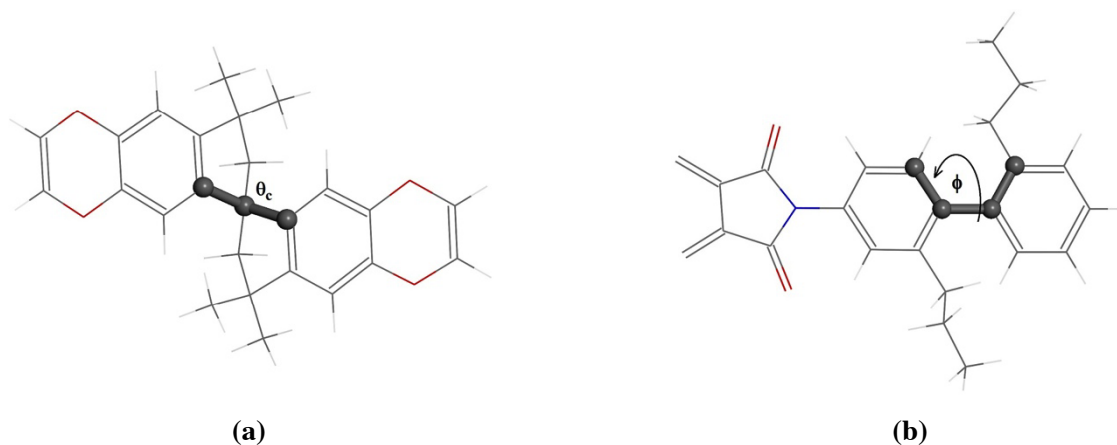
Figure 1. Schematic drawing of a portion of PIM molecule illustrating (a) the angle of contortion, θ_c, and (b) the torsional angle, ϕ, evaluated for the various polymeric structures.

Furthermore the torsional angle (ϕ) about the backbone bonds connecting the aromatic rings of a PIM molecule, figure 1b, is also evaluated to test the influence of the side groups of the polymeric structure on the restriction of the rotation around the polymeric backbone axis.
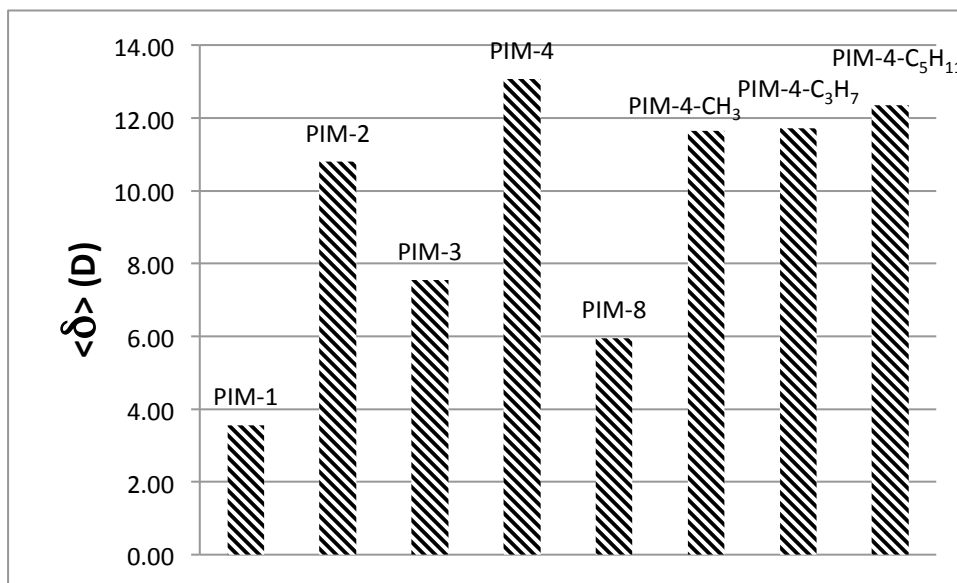
Figure 2. The influence of the molecular structure on the dipole moment of the PIM-polyimides.

3. Results and Discussion

The use of molecular simulation techniques allows for the modeling and investigation of the influences of the molecular structures on the conformational behavior of PIM-polyimides. Figure 2 illustrates the influence of the chemical structure of the various polymers listed in tables 1 and 2 on the dipole moment of these polymers.

It is obvious from the figure that the dipole moment of all the linear polymers, PIM-1, 3, 8 have low dipole moment despite the presence of the fluorine atoms in PIM-3, which obviously cancel each other to a large extent. Once the polymer exhibit non-linear backbone, the dipole moment increases sharply. Replacing in the fluorine atoms in PIM-4 with bulky alkyl groups didn't influence the dipole moment greatly indicating that the size of the side chains has much less dramatic influence than having a bent backbone such as in PIM-2 or the presence of alternating side chains on neighbouring aromatic rings.

Figure 3 illustrates the influence of the molecular structure on the radius of gyration of the PIM-polyimides. The figure clearly shows that all the PIMs have similar Rg values with the exception of PIM-2 due to the presence of the bent angle in the backbone which allows the polymeric chains to assume less extended configuration. PIM-3 also exhibited a low value for the radius of gyration, which can be explained on the basis of the presence of the tetrahedral carbon atom connecting the two phenyl group. Unlike, PIM-4 in which both phenyl rings lie on the same plane, the presence of the tetrahedral carbon atom between the two phenyl rings causes the bond angle of the C (ring 1) – C (tetrahedral atom) – C (ring 2) to be 109.5° causing an out-of-plane kink and a decrease in the radius of gyration as in the case of PIM-2 but to a lesser extent.

Figure 4 illustrates the influence of the molecular structure on the probability distribution function of the torsional angle (ϕ) of PIM-1, 2, 3 and 8. It is clear from the figure that the bulkiness and the bent backbone configurations of PIM-2 and 8 has caused the torsional angle to be limited to a narrow range around a certain value and unable to cross a potential energy barrier, hence the zero-value of the probability function for these two structures. Simple and linear backbone structures such as the case of PIM-1 and 3 showed the ability of the torsional angles to visit various angle and to cross the various low potential energy values.
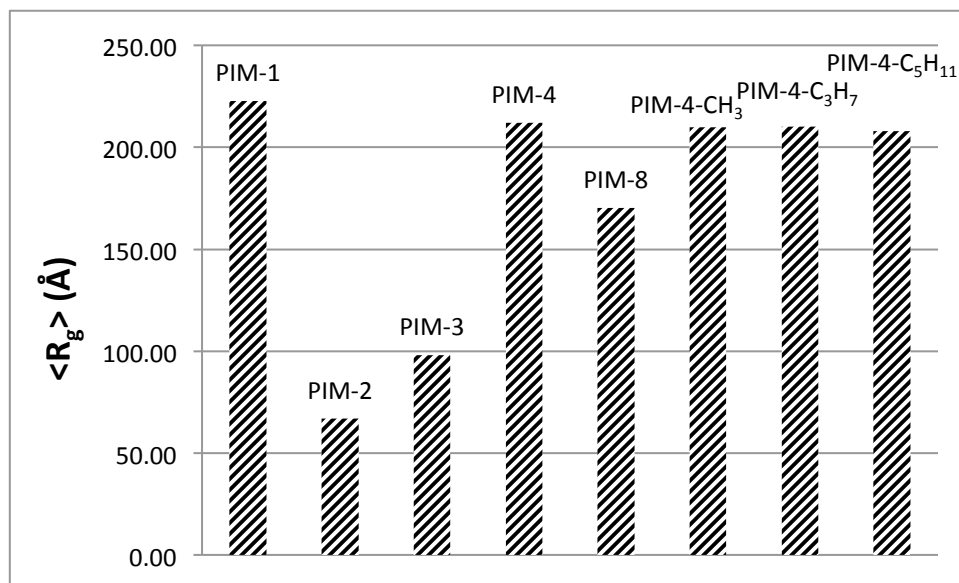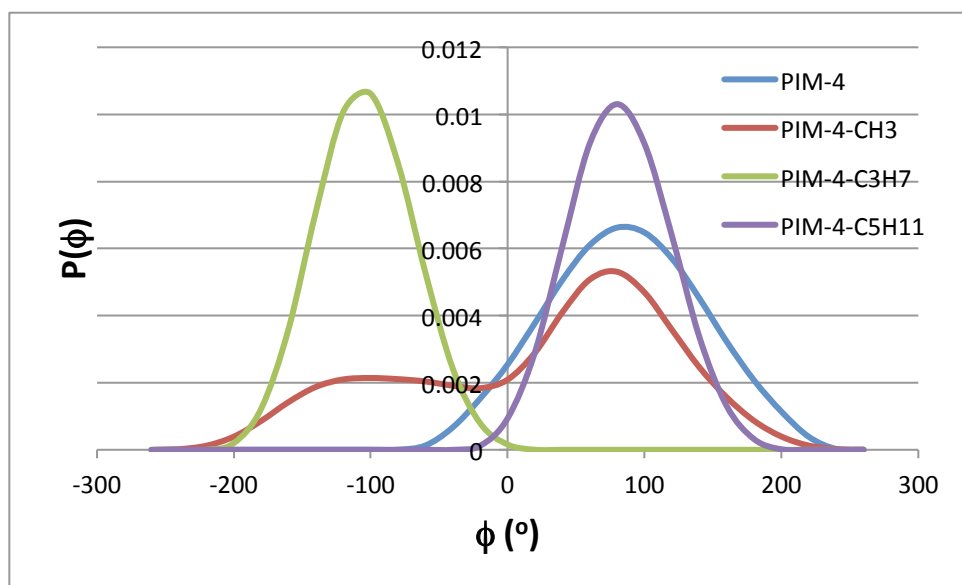
Figure 3. The influence of the molecular structure on the radius of gyration of the PIM-polyimides.

Figure 5 depicts the influence of the molecular structure on the probability distribution function of the torsional angle (ϕ) of PIM-4, 4-CH$_3$, 4-C$_3$H$_7$ and 4-C$_5$H$_{11}$. Similarly to the observation made in figure 4, the presence of the bulky side groups in PIM-4, 4-C$_3$H$_7$ and 4-C$_5$H$_{11}$ has caused the energy barriers of cis-configurations to increase dramatically, which prevents the polymeric segments from experiencing full rotation about the connecting bonds. To a lesser extent, this was observed for PIM-4-CH$_3$ due to the smaller size of the methyl group.
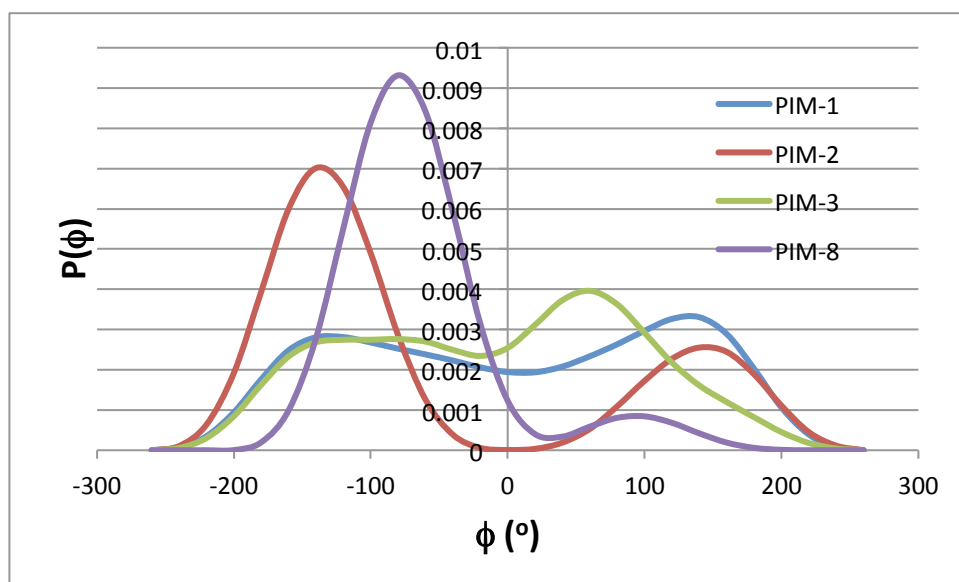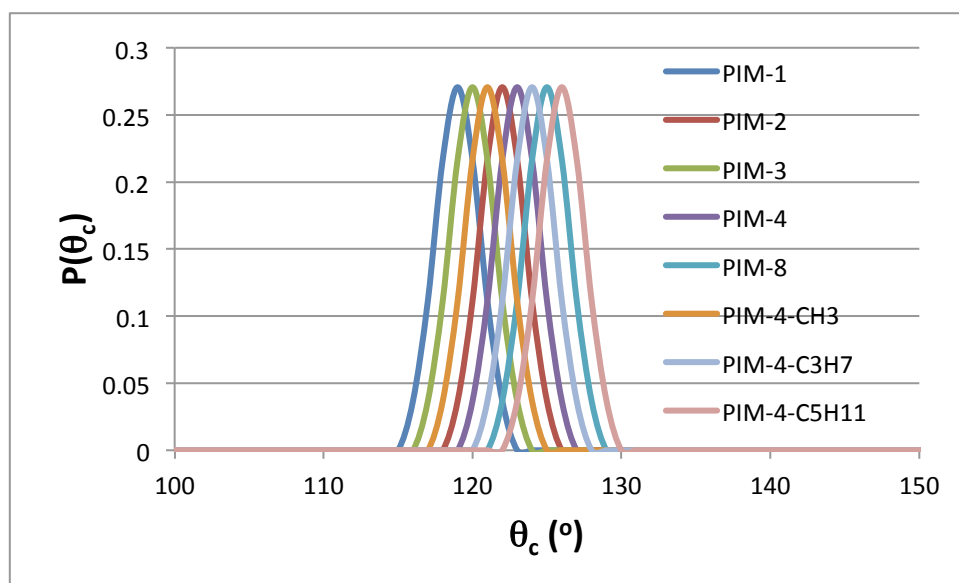

Figure 4. The influence of the molecular structure on the probability distribution function of the torsional angle (ϕ) of PIM-1, 2, 3 and 8.
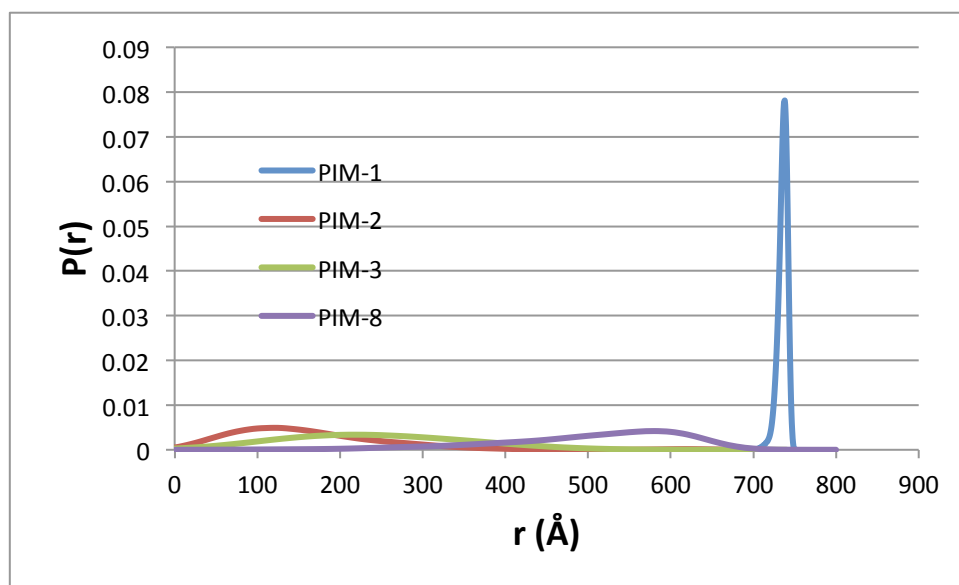
Figure 5. The influence of the molecular structure on the probability distribution function of the torsional angle (ϕ) of PIM-4, 4-CH$_3$.

Figure 6 shows the influence of the molecular structure on the probability distribution function of the angle of contortion (θ_c) of the PIM-polyimides. It is obvious from the figure that the contortion angle had a very limited range of bending due to the high steric hindrance around the sp^3 hybridized tertiary C-atom. Interestingly, the values of the probability distribution function itself didn't show much change with the variation of the molecular structure of the various polymers.

Figure 6. The influence of the molecular structure on the probability distribution function of the angle of contortion (θ_c) of the PIM-polyimides.

Figure 7. The influence of the molecular structure on the probability distribution function of the end-to-end distance (r) of PIM-1, 2, 3 and 8.

Figure 7 exhibits the influence of the molecular structure on the probability distribution function of the end-to-end distance (r) of PIM-1, 2, 3 and 8. It is rather interesting that the probability distribution functions showed a high value for PIM-1 and quite narrow variation in the value of the end-to-end distance. This indicates that fully extended configuration is the preferred configurations for these polymers in the absence of strong electronegative atoms, backbones kinks or bulky side groups. The addition of any of these factors to the polymeric structures results in the polymeric chains being forced to assume less extended configurations.
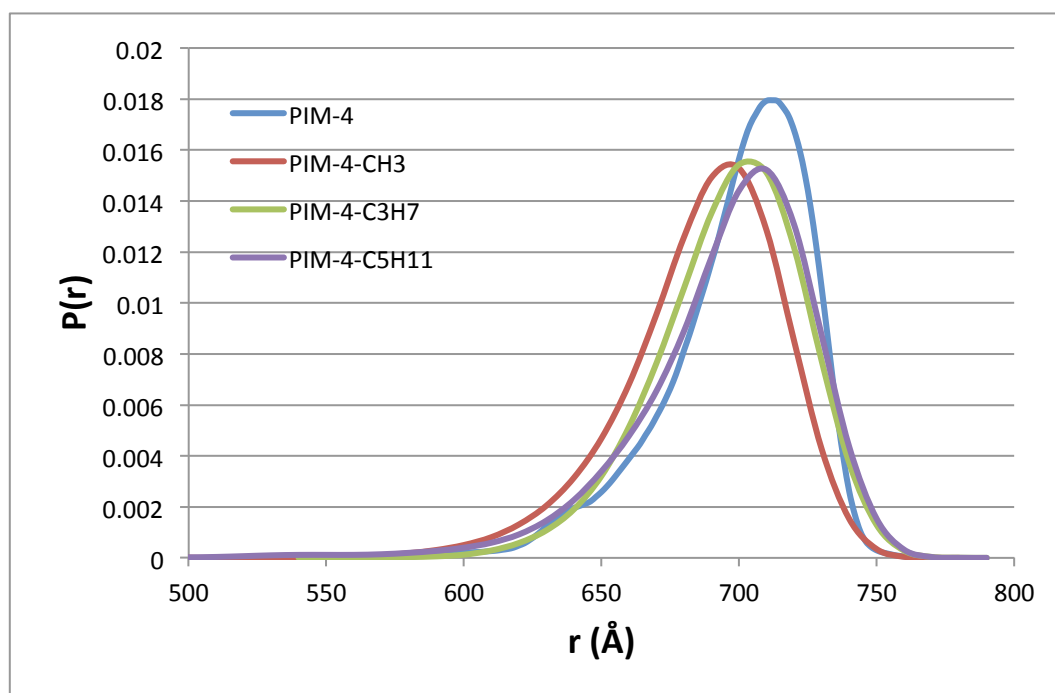
Figure 8 illustrates the influence of placing bulky side chains of different length on the probability distribution function of the end-to-end distance (r) of PIM-4, 4-CH_3, 4-C_3H_7 and 4-C_5H_{11}. Rather interstingly, the length or bulkiness of the side groups didn't affect the end-to-end distance distribution very much in clear agreement with the observations made earlier for the radius of gyration, figure 3.

Figure 9 exhimibts the influence of the molecular structure on the probability distribution function of radius of gyration of the PIM-polyimides. As discussed earlier, in the absence of side groups, electronegative atoms such as the fluorine atoms or backbone kinks, PIM-1 show the most preferred fully extended configuration with high value for both the end-to-end distance and the radius of gyration. The presence of these factors has caused the radius of gyration to assume various values in response to the polymeric chains assuming different configurations. Interesting, figure 9 predicts that the presence of quite large bulky side chain such as the pentyl group has caused the polymeric chains to revert back to the fully extended configurations possibly due to the quite high potential energy barriers that the chains have to cross to reach the less extended configurational states.

4. Conclusion
The use of molecular simulation techniques allows for the modeling and investigation of the influences of the molecular structures on the conformational behavior of PIM-polyimides of different molecular structures. Three factors obviously influenced the conformational behavior of these

polymers, which are the presence of electronegative atoms, the presence of non-linearity in the polymeric backbones (backbone kinks) and the presence of bulky side groups on the polymeric chains. The dipole moment increased sharply with the presence of backbone kinks more than any other factor. Replacing the fluorine atoms in PIM-4 with bulky alkyl groups didn't influence the dipole moment greatly indicating that the size of the side chains had much less dramatic influence on the dipole moment than having a bent backbone. Similarly, the presence of the backbone kinks in the polymeric chains influenced the polymeric chains to assume less extended configuration causing the torsional angles around the interconnecting bonds unable to cross the high potential energy barriers. The presence of the bulky side groups also caused the energy barriers of the cis-configurations to increase dramatically, which prevented the polymeric segments from experiencing full rotation about the connecting bonds. For these polymers, it was clear that the fully extended configurations are the preferred configurations in the absence of strong electronegative atoms, backbones kinks or bulky side groups. The addition of any of these factors to the polymeric structures resulted in the polymeric chains being forced to assume less extended configurations. Rather interestingly, the length or bulkiness of the side groups didn't affect the end-to-end distance distribution to a great deal since the presence of quite large bulky side chain such as the pentyl group has caused the polymeric chains to revert back to the fully extended configurations possibly due to the quite high potential energy barriers that the chains have to cross to reach the less extended configurational states.

Figure 8. The influence of the molecular structure on the probability distribution function of the end-to-end distance (r) of PIM-4, 4-CH_3, 4-C_3H_7 and 4-C_5H_{11}.

References

[1]   Lu G Q and Zhao X S 2004 *Nanoporous Materials: Science and Engineering* (London: Imperial College Press)
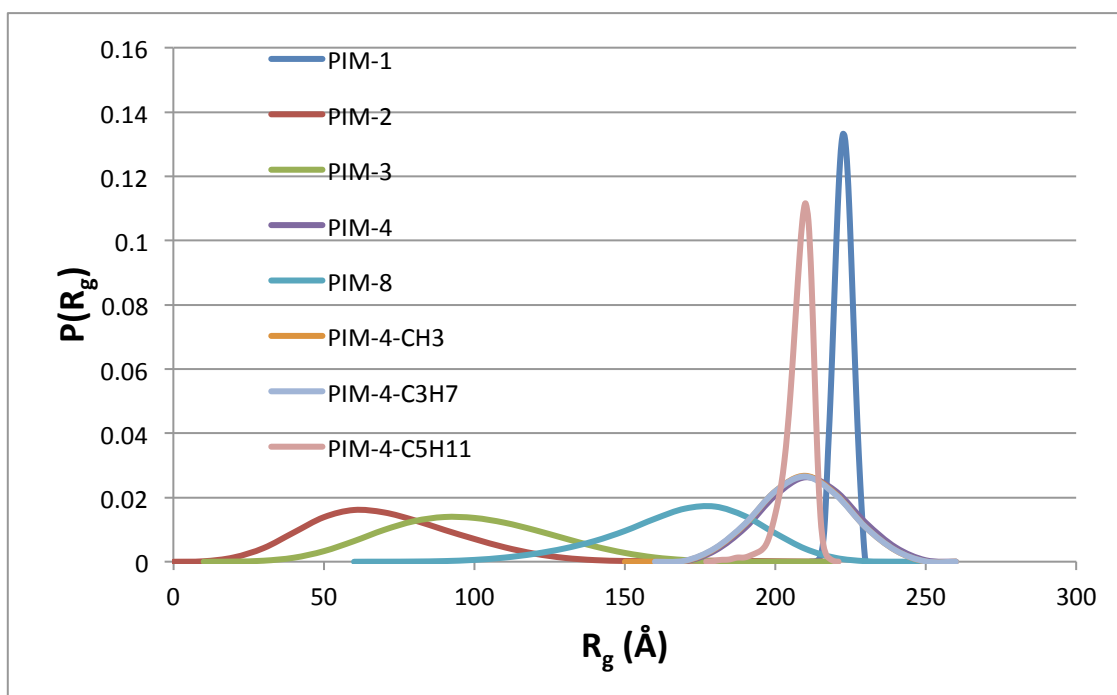
Figure 9. The influence of the molecular structure on the probability distribution functions of radius of gyration of the PIM-polyimides.

[2]   Bae T H 2010 *Engineering Nanoporous Materials for Application in Gas Separation Membranes* (Ph.D. thesis: Georgia Institute of Technology)

[3]   Madkour T and Mark J 1998 *Macromolecular Theory and Simulations* **7**, 69-77

[4]   Budd P M, Msayib K J, Tattershall C E, Ghanem B S, Reynolds K J, McKeown N B and Fritsch D 2005 *Journal of Membrane Science* **251** 263

[5]   Trewin A and Cooper A 2010 *Angew. Chem. Int. Ed.* **49** 1533

[6]   Ghanem B S, Mckeown N B, Budd P M, Selbie J D and Fritsch D 2008 *Advanced Materials* **20** (14) 2766

[7]   Madkour T and Mark J 2002 *J. Polym. Sci. Polym. Phys.* **40**(9) 840

[8]   McKeown N B, Budd P M and Book D 2007 *Macromol. Rapid. Commun.* **28** 995

[9]   Svec F, Germain J and Fréchet J M 2009 *Small* **5** 1098

[10]   McKeown N B and Budd P M 2006 *Chem. Soc. Rev.* **35** 675

[11]   Germain J and Fréchet J M 2008 *J. Chem. Mater.* **20** 7069

[12]   Ghanem B S, McKeown N B, Budd P M, Al-Harbi N M, Fritsch D, Heinrich K, Starannikova L, Tokarev A and Yampolskii Y 2009 *Macromolecules* **42** 7881

[16]   Madkour T and Mark J 1997 *Journal of Polymer Science Part B: Polymer Physics* **35**(**16**) 2757

[13]   Germain J B 2008 *Nanoporous Polymers for Hydrogen Storage and Sulfur as a thin-film Etch Resist* (PhD thesis: University of California, Berkeley)

[14]   Madkour T and Barakat A M 1997 *Computational and Theoretical Polymer Science* **7**(**1**) 35

[15]   Du X, Sun Y L, Tan B E, Teng Q F, Yao X J, Su C Y and Wang W 2010 *Chem. Commun.* **46** 970

[17]   Madkour T and Soldera A 2001 *European Polymer Journal* **37**(6), 1105

[18]   Madkour T, Azzam R and Mark J 2006 *J. Polym. Sci. Polym. Phys.* **44** 2524